NANO LETTERS

LETTER

pubs.acs.org/NanoLett

Oriented Catalytic Platinum Nanoparticles on High Surface Area Strontium Titanate Nanocuboids

James A. Enterkin,*[†,§] Kenneth R. Poeppelmeier,[†,§] and Laurence D. Marks[‡,§]

[†]Department of Chemistry, Northwestern University, 2145 Sheridan Road, Evanston, Illinois 60208, United States

[‡]Department of Materials Science and Engineering, Northwestern University, 2220 Campus Drive, Evanston, Illinois 60208, United States

[§]Institute for Catalysis in Energy Processes and Center for Catalysis and Surface Science, Northwestern University, 2137 Sheridan Road, Evanston, Illinois 60208, United States

ABSTRACT: Platinum nanoparticles grown on $SrTiO_3$ nanocuboids via atomic layer deposition exhibit cube-on-cube epitaxy with the predicted Winterbottom shape, consistent with literature values of the interfacial and surface free energies. This thermodyamically stable configuration should survive the rigors of catalytic conditions to create stable, high surface area, face-selective catalysts.

KEYWORDS: Nanoparticle catalysis, noble metal catalyst, platinum, strontium titanate, Wulff construction, Winterbottom construction

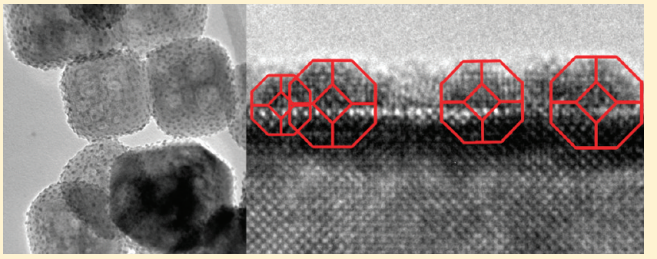

Because many industrial processes are dependent on catalysis, any advance in the design of catalysts can provide significant benefits to society. Although catalytic supports are often selected for their high surface area or thermal, chemical, and mechanical stability, the support can also affect the selectivity and reactivity of the catalyst.[1−3] Classic catalytic work, for example that of Sinfelt and co-workers,[4−7] has shown that changing the support can dramatically alter the catalytic behavior. Many theories have been proposed to explain the general role of supports, including sites at the metal−support interface,[8] particle size and surface-structure sensitivities,[9] ensemble-size sensitivity,[10] and strong metal−support interactions.[11,12] The latter includes concepts such as intermetallic bond formation and charge transfer,[13,14] diffusion of metal species between support and catalyst,[1,15,16] geometric decoration,[17−22] and other electronic effects.[23,24] These insights have been gained from studies on model systems, largely single crystals. In the past, the various surface facets on high surface area supports have made these insights difficult to exploit, although the use of a support with both high surface area and controlled orientation may offer the opportunity to bridge this gap.

One of the more intriguing aspects of support effects is the potential to stabilize a catalyst with the exposed faces carefully controlled. Such a catalyst would be able to take advantage of the differences in selectivity and reactivity of different faces as demonstrated in studies on oriented single crystals (see, for example, refs 25−27 and references therein). Catalysts dispersed on high surface area supports are normally found with a wide range of sizes, shapes, orientations, and surface structures. There have been many attempts to bridge this gap by creating high surface area nanoparticle catalysts with specific exposed surfaces but ultimately with little success. Even when a desired (surface) structure is created by some chemical kinetic path for the initial catalyst, it is a metastable configuration which will not survive catalytic conditions and will revert to the thermodynamically stable structure. This is true particularly if it contains higher energy more reactive surfaces such as face-center cubic {100}. Discovering or engineering a thermodynamically stable, high surface area, nanoparticle catalyst with designed exposed faces would be a significant step forward in catalytic research. Achieving precise control over which faces are predominantly exposed and in what ratios remains an important, ongoing challenge.

While at times separated from the catalytic community, much fundamental research has been conducted on the shape and orientation of metal nanoparticles. The shape of free metal nanoparticles has long been known to be governed by the Wulff construction[28] and that of supported metal nanoparticles the Winterbottom construction.[29] Indeed, even such complicated aspects as the structure of multiply twinned metal nanoparticles[30−33] are solved problems, and the surface structures of such metal nanoparticles is well understood.[34] While many of these studies were motivated by the potential of these types of particles for catalysis,[35,36] such insights have not been exploited in the design of catalysts.

Recent synthesis of high surface area oriented $SrTiO_3$ nanocuboids[37,38] opens up new possibilities. When used as a catalytic support, strontium titanate is in powder form without well-defined surface facets exposed. The $SrTiO_3$ nanocuboids

Received: October 23, 2010
Revised: January 24, 2011
Published: February 02, 2011

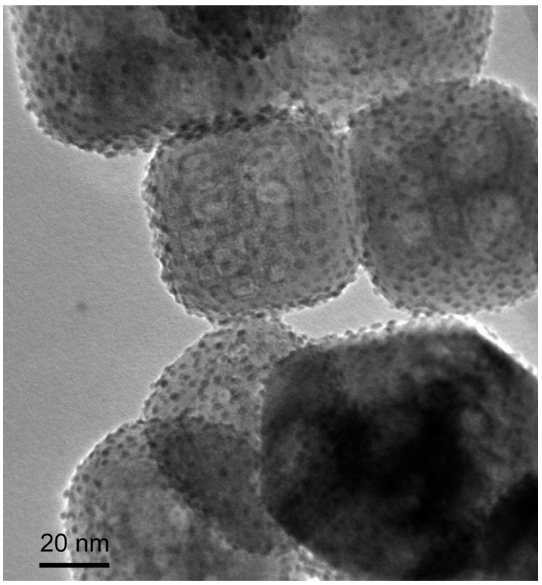

Figure 1. Low-resolution TEM image of platinum nanoparticles on strontium titanate nanocuboids.

have primarily the low energy {100} face exposed with a smaller amount of {110},[37] for which many details of the surface structure are available.[39−44]

We report here results on the structure of platinum nanoparticles grown on these $SrTiO_3$ nanocuboids and show that the nanoparticles have a strong cube-on-cube epitaxy with the predicted Winterbottom shape, consistent with literature values of the interfacial free energy as well as the surface free energy of $SrTiO_3${100}, Pt{100}, and Pt{111} surfaces. This is a *thermodyamically stable* shape which exposes different surfaces of the nanoparticles than those exposed when supported on polycrystalline supports. As such, we can expect this stable configuration to survive the rigors of catalytic conditions for extended periods of time. In effect we have engineered specific surfaces of the nanoparticles by combining thermodynamics with engineering of the support, and we propose that this concept is general and can be used to create stable, high surface area, face-selective catalysts.

Hydrothermally synthesized strontium titanate nanocuboids[37] with platinum nanoparticles deposited onto the surfaces via atomic layer deposition (ALD)[45] were used as received. As explained in more detail below, the resulting platinum nanoparticle shape is the thermodynamically stable shape, meaning that the method of deposition should not be a factor in determining particle shape. The major advantage of ALD would be fine control of the amount of platinum deposited.[45,46] In this study only samples with a single Pt ALD cycle were analyzed as they had the greatest separation of platinum particles. Electron microscopy analysis was carried out in a JEOL JEM-2100 operated at 200 kV.

Images showed that platinum particles approximately 1.5−2.5 nm in diameter were formed (Figure 1); for random orientations such as this and at low magnifications the platinum particles appear approximately circular and one cannot obtain directly interpretable information about their internal or external structure. High-resolution imaging shows that the particles are metallic Pt with the lattice fringes of the platinum nanoparticles aligned with those of the strontium titanate with cube-on-cube epitaxy. A strong epitaxy is not surprising, as the lattice mismatch between platinum and strontium titanate is only 0.4% (3.920 Å for platinum and 3.905 Å for strontium titanate). The platinum was observed to grow only in the ⟨100⟩ direction and not in the ⟨111⟩ direction, which implies that the $SrTiO_3$ nanocuboids were TiO_2 terminated.[47] Such interfaces are known to have strong Pt−O bonds between the metal and the oxide support.[47,48]

While these particles are unconditionally metallic platinum, for completeness we note there can be dissociative chemisorption of O_2 on exposure to air[49] forming a PtO monolayer at the surface, and there are Pt−O bonds at the interface to the $SrTiO_3$.[47,48] Hence bulk averaging techniques might interpret these nanoparticles as PtO. For example, a nanoparticle consisting of 4 unit cells of platinum arranged in a square on the substrate surface would have 38 platinum atoms, 29 at the surface, 13 at the support interface, leaving only 4 (10%) in the interior. Such a particle would have a length of 1.063 nm and a height of 0.670 nm, with 90% of the platinum bonded to an oxygen atom. This is consistent with results from Setthapun and co-workers,[46] who reported that after one cycle of Pt ALD on $SrTiO_3$ nanocuboids, the platinum nanoparticles were 5% metallic platinum and 95% PtO and after two cycles 45% metallic platinum and 55% PtO; as well as Christensen and co-workers,[45] who reported that the amount of oxidation scaled with surface to volume ratio.

The observed shape of the platinum particles matched the Winterbottom construction,[29] a modification of the Wulff construction[28] for particles on a substrate. In the Wulff construction (the thermodynamically stable shape) the length of a vector normal to a crystal face which connects that face with the origin is proportional to the surface free energy per unit area of that crystal face, as shown in Figure 2a using the literature $\gamma_{Pt\{111\}}/\gamma_{Pt\{100\}}$ of 0.84 from Vitos et al.[50] The Winterbottom construction is similar to the Wulff construction but includes the interface free energy between the particle and the substrate and the surface free energy of the substrate. The interface free energy can be written as

$$\gamma_{Int} = \gamma_{Pt} + \gamma_{STO} - \gamma_{Bond}$$

where γ_{Bond} is the free energy change per unit area associated with bonding across the interface, γ_{Pt} the surface free energy of the relevant Pt face, and γ_{STO} the surface free energy of the relevant $SrTiO_3$ face. This assumes that the $SrTiO_3$ surface is rigid and flat, which is not necessarily a correct assumption.[51] The Wulff shape will be truncated at a plane, the location of which is determined by the difference between the interfacial free energy and the substrate free energy (Figure 2b).[29]

On comparison of the amount of truncation in the experimental images to the Pt Wulff construction, it can be seen that slightly more than half of the Wulff shape was exposed above the substrate surface (Figure 3). Exactly half the particle would be exposed when the substrate surface energy and the interface energy are equal, i.e. $(\gamma_{interface} - \gamma_{substrate}) = 0$, while the entire Wulff construction would be exposed if the interface energy were greater than or equal to the particle surface energy plus the substrate surface energy, i.e., $(\gamma_{interface} - \gamma_{substrate}) \geq \gamma_{particle}$. Between 50% and 100% of the Wulff construction would be exposed when the interface energy is between the substrate surface energy and the substrate surface energy plus the particle surface energy, i.e., $0 < (\gamma_{interface} - \gamma_{substrate}) < \gamma_{particle}$.[29] The experimental data show that barely more than half of the particle is exposed; hence the interface energy is slightly greater than the substrate surface energy, consistent with previous literature reports.[52]

dx.doi.org/10.1021/nl104263j |*Nano Lett.* 2011, 11, 993–997

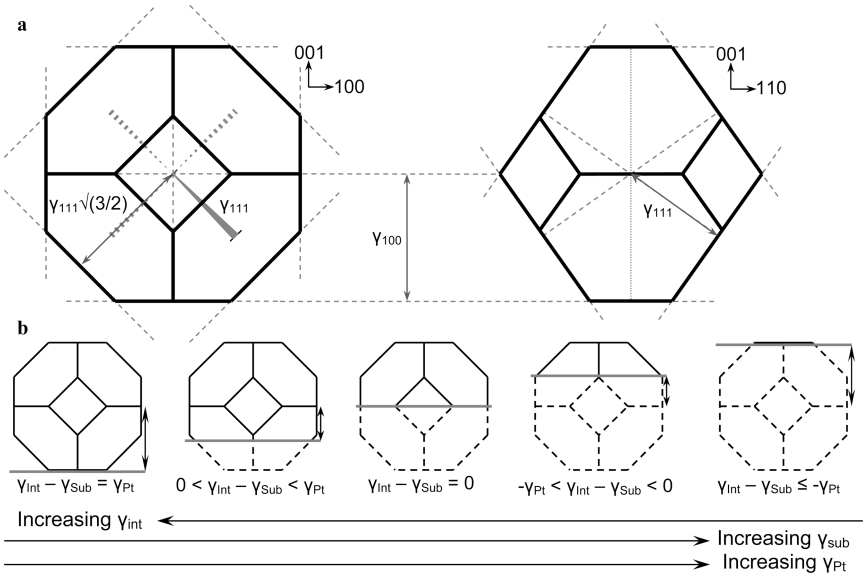

Figure 2. (a) Wulff construction[28] for platinum using the $\gamma_{\{111\}}$:$\gamma_{\{100\}}$ ratio of 0.84 from Vitos et al.[50] (b) Winterbottom construction[29] for platinum on a surface, showing relative energies for different possible degrees of truncation. Wulff shape in black, substrate surface in gray, with arrow indicating magnitude of $\gamma_{Int} - \gamma_{Sub}$.

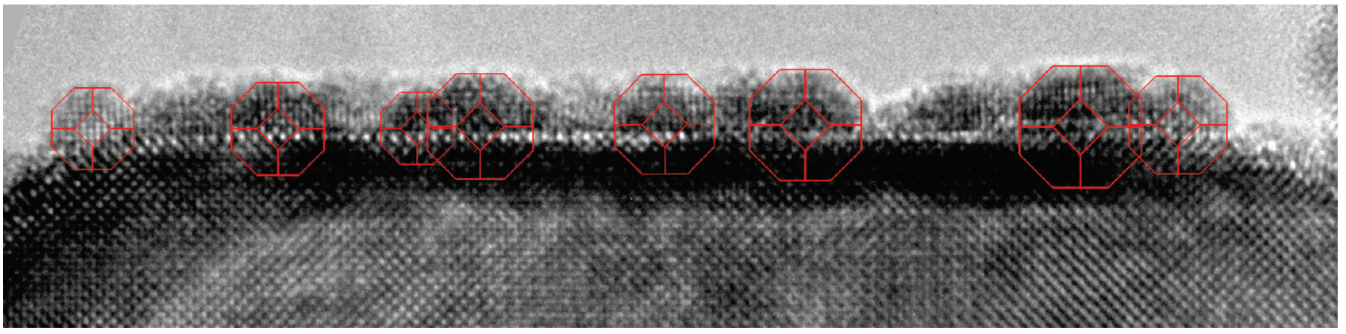

Figure 3. HREM image of platinum nanoparticles on the (100) face of a strontium titanate nanocuboid. The Pt particles can be differentiated from the $SrTiO_3$ substrate by both the difference in fringe spacings and the "white line" constrast at the $SrTiO_3$ surface in projection due to Fresnel imaging effects at the defocus used. Near perfect alignment of Pt{100} and $SrTiO_3${100} lattice fringes indicates a strong epitaxy. Wulff construction shapes for platinum are overlaid upon the platinum nanoparticles in red, showing that slightly more than half of the Wulff construction shape exists above the substrate surface.

The unreconstructed TiO_2 (1×1) termination for $SrTiO_3$ {100} has a surface free energy of 0.0582 eV/Å^2, calculated using the all-electron Wien2k code[53] with an augmented plane wave plus local orbital (APW+lo) basis set and the PBE generalized gradient approximation (GGA).[54] While the exact energy will vary dependent upon the reconstruction, other {100} titanium oxide rich terminations have similar energies. The absolute surface energies for the {111} and {100} surfaces of platinum calculated by Iddir et al. are 0.096 and 0.115 eV/Å^2, respectively.[52] From the experimental measurement of the platinum nanoparticle shape, the interface energy between the $SrTiO_3$ nanocuboids and the Pt nanoparticles is slightly greater than the $SrTiO_3$ {100} surface free energy. This is in good agreement with the GGA calculations by Asthagiri and Sholl, where the work of separation between Pt and the unreconstructed TiO_2 (1×1) terminated $SrTiO_3$ {100} was calculated to be 0.061−0.066 eV/ Å^2 for two to five monolayers of Pt,[48,55] and GGA calculations by Iddir et al., where the work of separation was calculated to be 0.066 eV/Å^2.[52]

On the basis of this evidence, we conclude that the observed shape of the platinum nanoparticles on the strontium titanate nanocuboids is the thermodynamically favored structure. Unlike metastable structures, which cannot survive extended catalytic use, thermodynamically stable structures such as these will be stable and maintain their configuration. Indeed, platinum in a different, metastable geometry will reconfigure to this thermodynamically stable shape.

The shape of the platinum nanoparticles is controlled by the interfacial free energy and the surface free energy of the support, changing these changes the ratio of exposed Pt{111} to Pt{100} which in turn will change face-selective catalytic performance. This is relatively simple to do, as perovskite nanocuboids of other compositions (e.g., $BaTiO_3$[56]) have also been synthesized, as have oriented nanoparticles of other materials (e.g., MgO smoke nanocubes[57,58]). For example, by switching to a support with a greater lattice mismatch for platinum ($a = b = c = 3.920$ Å) than $SrTiO_3$ ($a = b = c = 3.905$ Å; 0.4% lattice mismatch), such as $BaTiO_3$ ($a = b = 3.992$ Å, $c = 4.036$ Å; 2.2% lattice mismatch), the

dx.doi.org/10.1021/nl104263j |*Nano Lett.* 2011, 11, 993–997

interface energy would be expected to increase. This could be fine-tuned by having mixed ions on the A-site, e.g., $Sr_{1-x}Ba_x$-TiO_3. By changing the B-site cation, or by changing the material entirely, larger changes in the interface and substrate surface free energies will lead to associated changes in the exposed facets and face-selective catalysis.

As the particle shape is the thermodynamically favorable structure rather than a kinetic structure, it will be maintained during catalytic use, provided that the thermodynamics are not altered by poisoning or coking. (For completeness, the thermodynamical shape of relevance will be that for the specific gas and temperature conditions of the reaction, as chemisorption changes the Wulff-shape; see ref 59 and references therein.) Even if the particle size increases via sintering, the shape and the ratio of different surface facets will be maintained. Such a method for controlling a nanoparticle catalyst surface can be applied to any catalytic system, not just platinum, and manipulated as discussed above while maintaining thermodynamically stability. Our analysis of platinum nanoparticles on strontium titanate nanocuboids has illuminated a method by which stable, high surface area, oriented catalysts can be created.

Control of the support surface allows one to engineer such catalysts with precise control over what catalyst surface orientation is exposed, thus enabling precise modification of selectivity and yield for structure-sensitive catalytic reactions.

AUTHOR INFORMATION

Corresponding Author

*E-mail: j-enterkin@northwestern.edu.

ACKNOWLEDGMENT

The authors thank Federico Rabuffetti, Peter Stair, and Jeff Elam for providing the samples used in this analysis. This work was supported by the Northwestern University Institute for Catalysis in Energy Processing, funded through the US Department of Energy, Office of Basic Energy Science (Award Number DE-FG02-03-ER15457).

REFERENCES

(1) Haller, G. L.; Resasco, D. E. *Adv. Catal.* **1989**, *36*, 173–235.
(2) Verykios, X. E., Support Effects on Catalytic Performance of Nanoparticles. In *Catalysis and Electrocatalysis at Nanoparticle Surfaces*; Wieckowski, A., Savinova, E. R., Vayenas, C. G., Eds.; Marcel Dekker: New York, 2003.
(3) Coq, B.; Figueras, F. Effects of Particle Size and Support on Some Catalytic Properties of Metallic and Bimetallic Catalysts. In *Catalysis and Electrocatalysis at Nanoparticle Surfaces*; Wieckowski, A., Savinova, E. R., Vayenas, C. G., Eds.; Marcel Dekker: New York, 2003.
(4) Sinfelt, J. H. *J. Phys. Chem.* **1964**, *68* (2), 344.
(5) Taylor, W. F.; Yates, D. J. C.; Sinfelt, J. H. *J. Phys. Chem.* **1964**, *68* (10), 2962.
(6) Taylor, W. F.; Sinfelt, J. H.; Yates, D. J. C. *J. Phys. Chem.* **1965**, *69* (11), 3857.
(7) Yates, D. J. C.; Sinfelt, J. H.; Taylor, W. F. *Trans. Faraday Soc.* **1965**, *61* (513P), 2044.
(8) Hayek, K.; Kramer, R.; Paal, Z. *Appl. Catal., A* **1997**, *162* (1−2), 1–15.
(9) Che, M.; Bennett, C. O. *Adv. Catal.* **1989**, *36*, 55–172.
(10) Ponec, V. *Adv. Catal.* **1983**, *32*, 149–214.
(11) Tauster, S. J.; Fung, S. C.; Garten, R. L. *J. Am. Chem. Soc.* **1978**, *100* (1), 170–175.
(12) Tauster, S. J.; Fung, S. C.; Baker, R. T. K.; Horsley, J. A. *Science* **1981**, *211* (4487), 1121–1125.
(13) Dauscher, A.; Maire, G. *J. Mol. Catal.* **1991**, *69* (2), 259–270.
(14) Dauscher, A.; Muller, W.; Maire, G. *Catal. Lett.* **1989**, *2* (3), 139–144.
(15) Bond, G. C.; Rajaram, R. R.; Burch, R. *J. Phys. Chem.* **1986**, *90* (20), 4877–4881.
(16) Burch, R., Strong Metal-Support Interactions. In *Hydrogen Effects in Catalysis*; Paal, Z., Menon, P. G., Eds.; Marcel Dekker, Inc.: New York, 1988; p 347.
(17) Sadeghi, H. R.; Henrich, V. E. *J. Catal.* **1984**, *87* (1), 279–282.
(18) Simoens, A. J.; Baker, R. T. K.; Dwyer, D. J.; Lund, C. R. F.; Madon, R. J. *J. Catal.* **1984**, *86* (2), 359–372.
(19) Bernal, S.; Calvino, J. J.; Cauqui, M. A.; Cifredo, G. A.; Jobacho, A.; Rodriguez Izquierdo, J. M. *Appl. Catal., A* **1993**, *99* (1), 1–8.
(20) Ko, C. S.; Gorte, R. J. *J. Catal.* **1984**, *90* (1), 59–64.
(21) Logan, A. D.; Braunschweig, E. J.; Datye, A. K.; Smith, D. J. *Langmuir* **1988**, *4* (4), 827–830.
(22) Bernal, S.; Botana, F. J.; Calvino, J. J.; Lopez, C.; Perez Omil, J. A.; Rodriguez Izquierdo, J. M. *J. Chem. Soc., Faraday Trans.* **1996**, *92* (15), 2799–2809.
(23) Belzunegui, J. P.; Rojo, J. M.; Sanz, J. *J. Phys. Chem.* **1991**, *95* (9), 3463–3465.
(24) Belzunegui, J. P.; Sanz, J.; Rojo, J. M. *J. Am. Chem. Soc.* **1992**, *114* (17), 6749–6754.
(25) Spencer, N. D.; Schoonmaker, R. C.; Somorjai, G. A. *Nature* **1981**, *294* (5842), 643–644.
(26) Kohn, W.; Sham, L. J. *Phys. Rev.* **1965**, *140* (4A), A1133.
(27) Perdew, J. P.; Ruzsinszky, A.; Csonka, G. I.; Vydrov, O. A.; Scuseria, G. E.; Constantin, L. A.; Zhou, X. L.; Burke, K. *Phys. Rev. Lett.* **2008**, *100* (13), No. 136406.
(28) Wulff, G. *Z. Krystallogr. Mineral.* **1901**, *34* (5/6), 449–530.
(29) Winterbottom, W. L. *Acta Metall.* **1967**, *15* (2), 303.
(30) Marks, L. D. *Philos. Mag. A* **1984**, *49* (1), 81–93.
(31) Howie, A.; Marks, L. D. *Philos. Mag. A* **1984**, *49* (1), 95–109.
(32) Marks, L. D. *J. Cryst. Growth* **1983**, *61* (3), 556–566.
(33) Marks, L. D.; Smith, D. J. *J. Microsc. (Oxford, U.K.)* **1983**, *130* (May), 249–261.
(34) Marks, L. D.; Smith, D. J. *Nature* **1983**, *303* (5915), 316–317.
(35) Howie, A.; Marks, L. D.; Pennycook, S. J. *Ultramicroscopy* **1982**, *8* (1−2), 163–174.
(36) Marks, L. D.; Howie, A. *Nature* **1979**, *282* (5735), 196–198.
(37) Rabuffetti, F. A.; Kim, H. S.; Enterkin, J. A.; Wang, Y. M.; Lanier, C. H.; Marks, L. D.; Poeppelmeier, K. R.; Stair, P. C. *Chem. Mater.* **2008**, *20* (17), 5628–5635.
(38) Banerjee, S.; Kim, D. I.; Robinson, R. D.; Herman, I. P.; Mao, Y. B.; Wong, S. S. *Appl. Phys. Lett.* **2006**, *89* (22), 223130.
(39) Erdman, N.; Marks, L. D. *Surf. Sci.* **2003**, *526* (1−2), 107–114.
(40) Erdman, N.; Poeppelmeier, K. R.; Asta, M.; Warschkow, O.; Ellis, D. E.; Marks, L. D. *Nature* **2002**, *419* (6902), 55–58.
(41) Erdman, N.; Warschkow, O.; Asta, M.; Poeppelmeier, K. R.; Ellis, D. E.; Marks, L. D. *J. Am. Chem. Soc.* **2003**, *125* (33), 10050–10056.
(42) Lanier, C. H.; van de Walle, A.; Erdman, N.; Landree, E.; Warschkow, O.; Kazimirov, A.; Poeppelmeier, K. R.; Zegenhagen, J.; Asta, M.; Marks, L. D. *Phys Rev B* **2007**, *76* (4), No. 045421.
(43) Enterkin, J. A.; Subramanian, A. K.; Russell, B. C.; Castell, M. R.; Poeppelmeier, K. R.; Marks, L. D. *Nat. Mater.* **2010**, *9* (3), 245–248.
(44) Deak, D. S. *Mater. Sci. Technol.* **2007**, *23* (2), 127–136.
(45) Christensen, S. T.; Elam, J. W.; Rabuffetti, F. A.; Ma, Q.; Weigand, S. J.; Lee, B.; Seifert, S.; Stair, P. C.; Poeppelmeier, K. R.; Hersam, M. C.; Bedzyk, M. J. *Small* **2009**, *5* (6), 750–757.
(46) Setthapun, W.; Williams, W. D.; Kim, S. M.; Feng, H.; Elam, J. W.; Rabuffetti, F. A.; Poeppelmeier, K. R.; Stair, P. C.; Stach, E. A.; Ribeiro, F. H.; Miller, J. T.; Marshall, C. L. *J. Phys. Chem. C* **2010**, *114* (21), 9758–9771.
(47) Polli, A. D.; Wagner, T.; Gemming, T.; Ruhle, M. *Surf. Sci.* **2000**, *448* (2−3), 279–289.
(48) Asthagiri, A.; Sholl, D. S. *J. Chem. Phys.* **2002**, *116* (22), 9914–9925.

(49) Georgopoulos, P.; Cohen, J. B. *J. Catal.* **1985**, *92* (2), 211–215.
(50) Vitos, L.; Ruban, A. V.; Skriver, H. L.; Kollar, J. *Surf. Sci.* **1998**, *411* (1−2), 186–202.
(51) Ajayan, P. M.; Marks, L. D. *Nature* **1989**, *338* (6211), 139–141.
(52) Iddir, H.; Komanicky, V.; Ogut, S.; You, H.; Zapol, P. *J. Phys. Chem. C* **2007**, *111* (40), 14782–14789.
(53) Blaha, P.; Schwarz, K.; Madsen, G. K. H.; Kvasnicka, D.; Luitz, J. *WIEN2k, An Augmented Plane Wave Plus Local Orbitals Program for Calculating Crystal Properties*. Technical University of Vienna: Vienna, 2001.
(54) Perdew, J. P.; Burke, K.; Ernzerhof, M. *Phys. Rev. Lett.* **1996**, *77* (18), 3865–3868.
(55) Asthagiri, A.; Sholl, D. S. *Surf. Sci.* **2005**, *581* (1), 66–87.
(56) Miao, J.; Hu, C. G.; Liu, H.; Xiong, Y. F. *Mater. Lett.* **2008**, *62* (2), 235–238.
(57) Turkevich, J.; Hillier, J. *Anal. Chem.* **1949**, *21* (4), 475–485.
(58) Ardenne, M. v.; Beischer, D. *Angew. Chem.* **1940**, *53* (9−10), 103.
(59) Marks, L. D. *Rep. Prog. Phys.* **1994**, *57* (6), 603–649.